Investigation of the optical reflectivity of misfit layer compounds: $(MS)_nTS_2$(T=Ta, Nb; M=Sn, Pb, Sm, Tb, La; 1.08<n<1.23)

1994 J. Phys.: Condens. Matter 6 2117

(http://iopscience.iop.org/0953-8984/6/10/029)

J. Phys.: Condens. Matter 6 (1994) 2117–2128. Printed in the UK

Investigation of the optical reflectivity of misfit layer compounds: $(MS)_nTS_2$ (T=Ta, Nb; M=Sn, Pb, Sm, Tb, La; $1.08 < n < 1.23$)

C H Rüscher†, C Haas, S van Smaalen and G A Wiegers
Materials Science Centre, Laboratory of Chemical Physics, University of Groningen, Nijenborgh 16, 9747 AG Groningen, The Netherlands

Received 4 August 1993, in final form 15 November 1993

Abstract. The room temperature reflectivity of the misfit layer compounds $(MS)_nTS_2$ (T = Nb, Ta) is investigated in the spectral range 1000–20 000 cm^{-1}, The reflectivity for the E-vector parallel to the (001) planes and the incident light along [001] is dominated by the charge carrier response. This part of the spectra can be described using the Drude formula with the plasma frequency given by $\omega_p = (Ne^2/\epsilon_0\epsilon_\infty m^*)^{0.5}$ (N = charge carrier concentration, m^* = effective mass, ϵ_∞ = high-frequency dielectric constant). For compounds with M = Sn, Pb the number of charge carriers is equal to that of the parent compound TS_2. The observed anisotropy in the (001) plane is rather small and can be related to small differences in the effective masses ($m^*_{[010]}/m^*_{[100]} \simeq 0.98$). This effect is attributed to the orthorhombic distortion of the (TS_2) sublattice. For compounds with M = La, Sm, Tb, electron donation is indicated and the plasma frequency is determined by about 0.5, 0.2, 0.25 holes per T ion, respectively, in a single (TS_2)-related conduction band.

1. Introduction

The misfit layer compounds (MLCs) are a new class of compounds, with the chemical composition $(MS)_nTS_2$. For M, ions such as Sn, Pb, Bi or rare earth metals are usually incorporated, while T is mostly given by Nb, Ta or Ti. In addition to the class of materials with S anions, similar compounds are also known for Se. MLCs were first prepared around 1970 [1–7], but not recognized as such, an exception being $(LaS)_{1.2}CrS_2$ [8] for which the misfit layer character was established by single-crystal x-ray diffraction. The structures of the MLCs are characterized by an alternate stacking of the layers MS and TS_2 and are, therefore, often described as so-called intergrowth or composite structures. Hence, a common property of the class of structures of the MLCs is the presence of two or more, mutually incommensurate, three-dimensional lattices (e.g. [9–17]). The incommensurability of the length ratio of the two a axes (the a axes are parallel to each other), i.e. the misfit between the two hypothetical lattices, determines n (typically $1.08 < n < 1.23$), the chemical composition as given by $(MS)_nTS_2$.

The electrical transport and magnetic properties of the MLCs have been found to be strongly related to those of 2H-TaS_2, 2H-NbS_2 or 1T-TiS_2 (e.g. [11, 18–22], [23] and references therein), respectively. The electrical resistivity shows strongly anisotropic behaviour and is up to four orders larger for the electrical field directed perpendicular to

† Address to which correspondence should be sent: Institut für Mineralogie der Universität Hannover, Welfengarten 1, D-30167 Hannover, Germany.

0953-8984/94/102117+12$19.50

the layers ($E^{\perp}(001)$ plane) compared with the case $E\|(001)$. For $E\|(001)$ typical values for the resistivity are $(1–5)\times10^{-7}\Omega$ m below about 20 K, increasing linearly to about $(8–20)\times10^{-7}\Omega$ m at 300 K for the MLCs with T = Nb or Ta. Somewhat more complex T" behaviour is observed for the $(MS)_nTiS_2$ type of compounds [22]. Hall effect data for MLCs with T = Nb, Ta and M = Sm, Pb point to a slight electron donation from the MS layers into the half-filled (Nb, Ta)$S_2d(z^2)$ conduction band. For the Nb, Ta compounds with M = La, Tb, Sm significantly larger electron donation is indicated.

The Drude theory of free electrons in metals predicts a change in spectral behaviour from high reflectivity to transparency below and above the plasma frequency (ω_p), which is mainly determined by the number of free carriers. For $\omega < \omega_p$ the reflectivity is dominated by the scattering mechanism. Above ω_p the response is given by the effective dielectric constant. Hence in cases of no superposition by additional absorption and an ordinary scattering mechanism the carrier concentration can be calculated most easily using the reflectivity spectra. The measurement of reflectivity can thus provide additional information on the free carrier properties of the MLCs. This method has been used by several authors, e.g. to observe the doping effect by intercalation of 3d transition metals in 2H-NbS_2 and 2H-TaS_2 [24] or Ag in TiS_2 [25]. In this paper results from the study of the optical reflectivity of the MLCs are outlined. This paper is restricted to the charge carrier response observed for $E\|(001)$, i.e. for the electrical field vector directed parallel to the crystal plane along the layers, and to compounds with $TS_2 = NbS_2$ or TaS_2. It is shown that this type of structure possesses a small anisotropic effect for E rotated within this plane (here for $(PbS)_{1.13}TaS_2$). The assumption of charge transfer into the half-filled d conduction band of Nb and Ta compounds, with M = La, Sm, Tb, is strongly supported by the present results. It may be noted that the anisotropic effect in the reflectivity with respect to the $E^{\perp}(001)$ direction [26] corroborates the high anisotropy obtained in the resistivity for the MSCs. However, this feature will not be considered further here.

2. Experimental

The compounds of concern in this study are given in table 1, together with their lattice constants and references, where the route of preparation and characterization (structure refinements, chemical composition) are described [9, 10, 13, 19, 21, 27–31]. Crystals suitable for optical measurements were grown by vapour transport in a temperature gradient (typically 850–750 °C for M = Sn, Pb; 1150–760 °C for rare earth compounds) using halogen as the transport agent in evacuated quartz glass ampoules. The products have been checked using powder x-ray diffraction. They yield the intrinsic pattern expected for the various types of composition used here. Crystals yield in nearly all cases a plate-like shape with an irregular format of the layers, with maximal sizes of about 2×3 mm^2 and 20–80 μm in thickness (see e.g. [11]). Species were selected from each batch and glued with their flat side (001) to the sample holder. The surfaces of the sample were cleaned by stripping away several layers. The reflection spectra were then measured using a FTIR spectrometer equipped with an infrared microscope (Bruker IFS88, A590) and with an Au grid (KRS5) and prism (Glan Thompson K) polarizers for the incident light. The use of a microscope has the advantage of the possibility of using small spot sizes (here $d = 90$ μm). Suitable areas of the crystal for this investigation can easily be detected. The disadvantage is the focusing optic, which gives an angle of incidence of 15°. However, this does not seriously affect the results presented here [26]. The absolute value for the reflectivity was calculated using alternatively uncoated Ag and Al mirrors together with $SrTiO_3$ for calibration. The

Table 1. Lattice parameters (in Å) and unit-cell volume per formula unit (V_{fu} in Å^3) of the misfit layer compounds of concern in this study. a_1 and a_2 denote the a axis parameters for the TS_2 and MS parts, respectively. More details about the structure refinements are given in the references as listed. (Compare also the collection of data in [23].) For comparison the lattice parameters of 2H-NbS_2 and 2H-TaS_2 are also given.

Composition	a_1	a_2	b	c	V_{fu}	Ref.
$(PbS)_{1.14}NbS_2$	3.313	5.834	5.801	23.80	114.35	[13]
$(SnS)_{1.17}NbS_2$	3.321	5.673	5.751	11.76	112.31	[10]
$(TbS)_{1.21}NbS_2$	3.310	5.467	5.695	11.18	105.38	[23,27]
$(PbS)_{1.13}TaS_2$	3.304	5.825	5.779	23.96	114.37	[19]
$(SnS)_{1.16}TaS_2$	3.316	5.720	5.742	23.76	113.11	[9,28]
$(LaS)_{1.13}TaS_2$	3.295	5.813	5.775	11.53	109.70	[13]
$(SmS)_{1.19}TaS_2$	3.293	5.552	5.679	22.50	105.19	[21]
2H-NbS_2, $a = 3.31$–3.32, $c = 11.94$, $V_{fu} = 56$–57 ($P6_3/mmc$, [29,30])						
2H-TaS_2, $a = 3.314$, $c = 12.10$, $V_{fu} = 57.53$ ($P6_3/mmc$, [31])						

accuracy shows satisfactory results within 5% absolute deviations. However, the relative accuracy is better than 0.5%.

3. Results and discussion

3.1. Misfit layer compounds with M = Sn, Pb and T = Nb, Ta: the in-plane anisotropy

Typical spectra obtained for $(PbS)_{1.13}TaS_2$ and $(PbS)_{1.14}$ NbS_2 are given in figures 1 and 2. Also shown are the results from least-square fits of the Drude free carrier model with the real and imaginary part of the dynamic dielectric function

$$\epsilon'(\omega) = \epsilon_\infty(1 - \omega_p)^2/(\omega^2 + \gamma^2) \qquad \epsilon''(\omega) = \epsilon_\infty y\omega_p^2/\omega(\omega^2 + \gamma^2) \tag{1}$$

via

$$R(\omega) = [(n-1)^2 + k^2]/[(n+1)^2 + k^2] \tag{2}$$

where $n^2 = 0.5 \times [(\epsilon'^2 + \epsilon''^2)^{0.5} + \epsilon']$, $k^2 = 0.5 \times [(\epsilon'^2 + \epsilon''^2)^{0.5} - \epsilon']$, ω_p is the screened plasma frequency, γ = the damping constant, ϵ_∞ the high-frequency dielectric constant, and ω the angular frequency. All the spectra (see also figures 3–7) are given as a function of wavenumber in units of cm^{-1}. For convenience ω_p and γ are thus also given in units of cm^{-1} ($w = \omega/2\pi c$, $w_p = \omega_p/2\pi c$, $y = \gamma/2\pi c$; c = velocity of light).

It is important to note that the model has only been fitted to the data between the low-frequency limit to slightly above the reflectivity minima at w_0, leaving ϵ_∞, y and w_p as free parameters. Hence the fit is governed by w_0 and the line shape (i.e. y) below w_0. Further extension of the data used for the fit towards higher wavenumber largely reduces the quality of the fit below w_0. This is easily understood because above about 8000 cm^{-1} the reflectivity is strongly affected by interband transitions. Similar behaviour is well known from transmission and reflection investigations of various dichalcogenides (e.g. [24,32–35]). No attempt was made to resolve these absorption features, e.g. by combined Drude–Lorentz fits, because for the purpose of this study these absorption effects might be neglected. Kramers–Kronig analysis is also not used, because for a successful analysis the

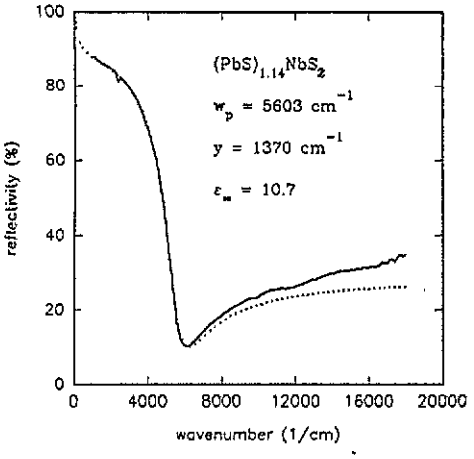

Figure 1. The reflectivity of the misfit layer compound $(PbS)_{1.14}NbS_2$ (full curve) and the Drude spectrum (dotted curve) with fit parameters as denoted.

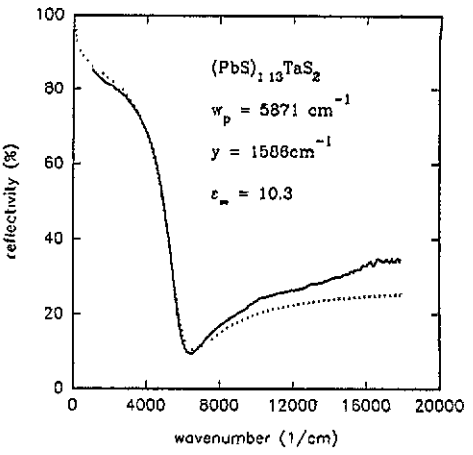

Figure 2. The reflectivity of the misfit layer compound $(PbS)_{1.13}TaS_2$ (full curve) and the Drude spectrum (dotted curve) with fit parameters as denoted.

spectra have to be extended far above the upper limit shown here, which is not necessary for the present purpose.

It has been observed that for $(SnS)_{1.16}TaS_2$ and $(SnS)_{1.17}NbS_2$ (not shown here) the Drude fit cannot be done with similar satisfactory results as obtained for the PbS compounds, indicating more of an influence from the underlying absorption. However, a qualitatively similar line shape as shown for the PbS MLCs is observed. For the SnS MLCs the plasma frequency can be expected to be in the same range as obtained for the PbS compounds (see the discussion in section 3.2 and table 3). It has also been observed that the position of the reflectivity minimum, i.e. the plasma frequency, varies slightly within a few per cent ($< 5\%$) for different samples of the same nominal chemical composition. This effect can be explained by a small variation in the stoichiometry from sample to sample.

The misfit layer compounds under study also show anisotropic reflection behaviour in the (001) plane. A typical example, which demonstrates this anisotropy for a $(PbS)_{1.13}TaS_2$ sample, is given in figures 3 and 4. In figure 3 spectra are plotted for the maximum and minimum position in the reflection minimum (w_0) in the spectral range 4000–8500 cm^{-1}. The spectrum with the higher w_0 belongs to the [010] lattice direction. The spectrum with the lower w_0 is representative of the electrical field vector for the incident light polarized parallel to the incommensurate lattice direction. Figure 4 details the relative change of the spectra by plotting the ratio of $(R(\theta)/R_{\theta=0})$, i.e. the ratio of the angle-dependent reflectivity ($R(\theta)$) with respect to the reflectivity with the lowest value for w_0 (i.e. $R_{\theta=0}$). Qualitatively similar results were also obtained for $(SnS)_{1.16}TaS_2$, $(SnS)_{1.17}NbS_2$ and $(PbS)_{1.14}NbS_2$. The angle-dependent variation of the intensity follows the dependence

$$R(\theta) = R_0 \cos^2\theta + R_{\pi/2} \sin^2\theta \tag{3}$$

with R_0 and $R_{\pi/2}$ being the main components of the reflectivities. In order to describe this anisotropy Drude fits are used. The obtained spectra, fitted to the experimental data points for the two extrema are given in figure 3. All fit parameters, including the results obtained for the experimental curves with $\theta = 30°$ and 60°, which give equally satisfying fit qualities as observed for the spectra shown, are listed in table 2. The results show that

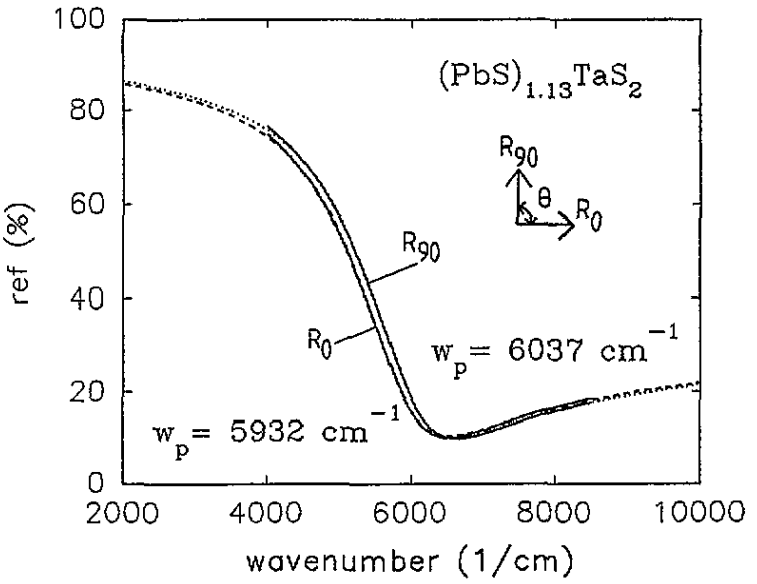

Figure 3. The resolved anisotropy for the spectral range 4000–8500 cm^{-1} (full curve) with results for the Drude fit. θ denotes the angle of rotation of the (001) crystal surface with respect to the direction of polarization of the incident light. R_0 denotes the spectra observed for the electrical field polarized parallel to [100], i.e. the incommensurate direction. R_{90} denotes the electrical field polarized parallel to [010].

the high-frequency dielectric constant (ϵ_∞) and the damping parameter (γ) remain stable, while w_p increases with θ by about 100 cm^{-1} (2%). It should be noticed that w_0, and hence w_p, are largely unaltered on varying absolute values for the reflectivity within the limits of accuracy ($\simeq$ 5%). This certainly affects ϵ_∞ and γ and explains, therefore, the larger uncertainty in the accuracy of absolute values for these parameters. On the other hand the angle dependence can be related to a variation in the effective mass via the Drude law.

$$\omega_p = (Ne_2/\epsilon_0 m^* \epsilon_\infty)^{0.5} \tag{4}$$

($\epsilon_0 = 8.85 \times 10^{-12}$ A s V^{-1} m^{-1}). Accordingly the results indicate an increased optical mass for carriers along the incommensurate lattice direction. However, the (small) anisotropic effect can be understood, e.g. within a simple tight-binding model, for the TS_2 sublattice alone, considering the TS_2 sublattice as a distorted hexagonal lattice (i.e. here $b > a_1\sqrt{3}$) with lattice parameters a_1 and b (see table 1). The effective masses are given by

$$m_x^* = h^2/3J_x a_1^2 \qquad \text{and} \qquad m_y^* = h^2/J_y b^2 \tag{5a,b}$$

(where J is the overlap integral), respectively, for the orthogonal directions. Therefore, for $PbS_{1.13}TaS_2$ a ratio in the effective masses related to the TS_2 sublattices is given by

$$m_y^*/m_x^* \simeq 0.98 \tag{6}$$

assuming $J_x \simeq J_y$. Accordingly the ratio w_{px}/w_{py} can be expected to be about 0.99, which should be compared with the observed value of 0.98. It may be noted that the true overlap integrals may slightly change the ratio (equation (6)) due to the orthorhombic distortion.

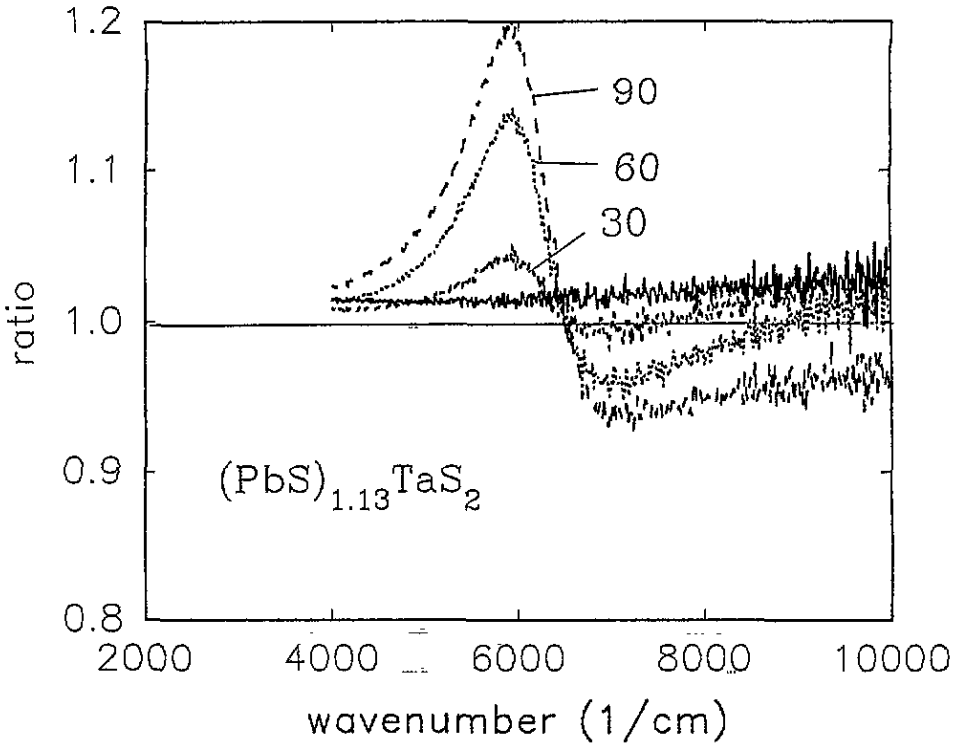

Figure 4. The ratio of reflectivity at $\theta = 30°$, 60° and 90° relative to the minimum position of the reflectivity (0°, see text), compared with the zero line and the spectra relative to the 180° position.

Table 2. Angle dependencies of Drude fit parameters (equations (1), (2), (4)) from the minimum to the maximum position of the minimum in the reflectivity of $(PbS)_{1.13}TaS_2$ (w_p, y in cm^{-1}).

	0°	30°	60°	90°
w_p	5932	5951	6004	6037
ϵ_∞	11.67	11.81	11.71	11.64
y	1349	1341	1345	1324

3.2. Electron donation in misfit layer compounds with M = La, Sm, Tb: the possibility of charge transfer

The reflection spectra obtained for $(LaS)_{1.13}TaS_2$, $(SmS)_{1.19}TaS_2$ and $(TbS)_{1.21}NbS_2$ are shown in figures 5, 6 and 7, respectively. Also shown are the results for the appropriate Drude fits. In section 3.1 it has been discussed that the uncertainty in the absolute value for the reflectivity mainly determines the precision obtained for the high-frequency dielectric constant (ϵ_∞), beside the superposition by other excitations (i.e. band–band excitations above about 8000 cm^{-1}). It is argued that ϵ_∞ may be obtained from the Drude fit describing the effective contribution from electronic transitions above the plasma edge threshold. For the compounds with M = La, Sm and Tb, systematically lower ϵ_∞ values ($\epsilon_\infty \simeq 8$–9) compared with the MLCs with Pb ($\epsilon_\infty \simeq 10$–12) are observed. It is also indicated, by the fitted data,

that the scattering mechanism is different for the La, Sm and Tb compounds, i.e. the optical damping constant appears to be reduced compared with the Pb and Sn MLCs.

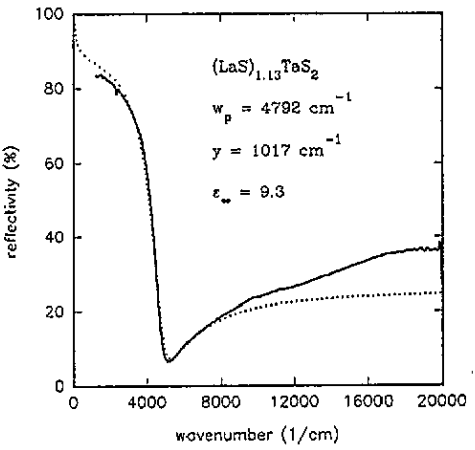

Figure 5. The reflectivity of the misfit layer compound $(LaS)_{1.13}TaS_2$ (full curve) and the Drude spectrum (dotted curve) with fit parameters as denoted.

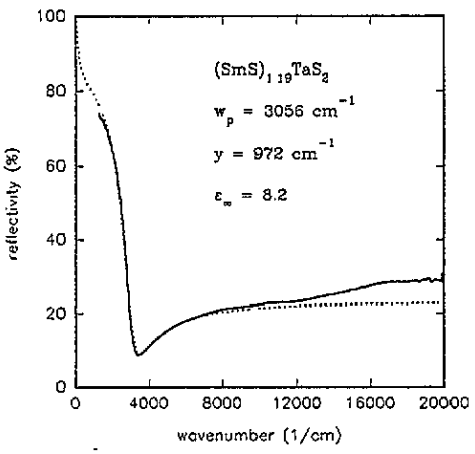

Figure 6. The reflectivity of the misfit layer compound $(SmS)_{1.19}TaS_2$ (full curve) and the Drude spectrum (dotted curve) with fit parameters as denoted.

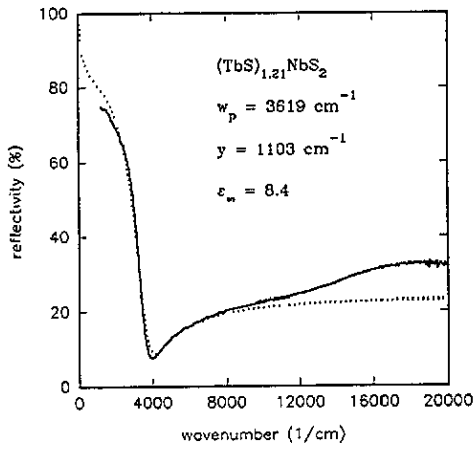

Figure 7. The reflectivity of the misfit layer compound $(TbS)_{1.21}NbS_2$ (full curve) and the Drude spectrum (dotted curve) with fit parameters as denoted.

The calculated plasma frequencies (and w_0) for these compounds appear to be certainly smaller than those obtained for $(PbS)_{1.14}NbS_2$ (see figure 2) and $(PbS)_{1.13}TaS_2$ (see figures 1 and 3). It has not yet been checked with higher accuracy by how much the anisotropy affects these results for the MLCs with La, Sm and Tb. The observability might also be largely reduced in these cases, because of the ability of orientation variants. However, using the results obtained in the last section concerning the ratio in the lattice constants, angle-dependent variations of w_p (w_0) can be expected within less than about 5%. Uncertainties,

which might be related to deviations from ideal stoichiometry, can also be assumed to be smaller than 5%. Therefore, the effect of different charge carrier concentration, *i.e.* doping by charge transfer of electrons from La, Sm, and Tb into the conduction band, considered to be mainly given by NbS_2/TaS_2, is a possible explanation for the reduction in w_p for these types of compounds, as will be shown in the following.

Table 3. Columns 1–3, used Drude fit parameters (w_p, ϵ_∞) and the calculated carrier concentration N_{exp} (equation (4) $m^* = 1$); columns 4 and 5, the theoretical carrier concentration N_{th} for a half-filled d_z^2 band of the NbS_2, TaS_2 subsystem ($m^* = 1$, see text) and the ratio $m_r = N_{th}/N_{exp}$ (in brackets, N_{th}/N_{est}) for the misfit layer compounds as given; columns 6–8, the observed minimum in the reflectivity (w_0), estimated plasma frequency $w_p \simeq 0.94 \times w_0$ (see text) and carrier concentration N_{est}. (N_{est}, N_{exp} and N_{th} are in units of 10^{27} m^{-3}; w_p, w_0 in cm^{-1}; 2nd, anisotropy resolved; *, not resolved; R_0 and R_{90} concern the anisotropy (compare figure 3).)

	1	2	3	4	5	6	7	8
Composition	w_p	ϵ_∞	N_{exp} $m^* = 1$	N_{th} $m^* = 1$	m_r	w_0	$w_p \simeq$	N_{est}
$(PbS)_{1.14}NbS_2$	5801	10.7	3.7	8.7	2.3	5900–6400	5546–6016	3.4–4.0
(2nd): (R_0)	5448	10.9	3.6	8.7	2.4			
(R_{90})	5528	11.3	3.8	8.7	2.3			
$(SnS)_{1.17}NbS_2$	*	*	*	8.9	(2.5)	6000	5640	3.5
$(TbS)_{1.21}NbS_2$	3619	8.4	1.2	9.5	7.9	3900	3666	1.5
$(PbS)_{1.13}TaS_2$	5871	10.3	3.9	8.7	2.2	6200–6400	5828–6016	3.7–4.0
(2nd): (R_0)	5932	11.7	4.5	8.7	1.9			
(R_{90})	6073	11.6	4.7	8.7	1.8			
$(SnS)_{1.16}TaS_2$	*	*	*	8.8	(1.9)	6850	6439	4.6
$(LaS)_{1.13}TaS_2$	4792	9.3	2.3	9.1	3.9	5100	4794	2.5
$(SmS)_{1.19}TaS_2$	3056	8.2	0.84	9.5	11.3	3380	3177	1.1
2H-NbS_2 [24]	*	*	*	17.7	(2.30)	8900	8366	7.7
2H-NbS_2 [36]	*	*	*	17.7	(2.45)	8600	8084	7.2
2H-TaS_2 [24]	*	*	*	17.4	(1.6)	10 500	9870	10.7

All data obtained from the Drude fits, including those of the last paragraph, are collected in table 3. Also listed are the observed carrier concentrations (N_{exp}) calculated using the experimental data, together with equation (4), and with the assumption that $m^* = 1$. For the sake of comparison the positions of the minimum in the reflectivities (w_0) are then listed together with known data for 2H-NbS_2 and 2H-TaS_2, as given by Parkin and Beal [24] and our own results for 2H-NbS_2 [36] for w_0. Also given are values obtained for $(SnS)_{1.17}NbS_2$ and $(SnS)_{1.15}TaS_2$ [36]. These data are used for an estimate of the plasma frequency as given by [37]

$$w_p = w_0[(\epsilon_\infty - 1)/\epsilon_\infty]^{0.5} \tag{7}$$

with $\epsilon_\infty = 10$. The carrier concentrations due to the so-estimated plasma frequencies are also listed in table 3. It is observed that the carrier concentration from the fitted data and those estimated using equation (7) agree fairly well. Therefore, the values for 2H-NbS_2 and 2H-TaS_2 may also be given further consideration. For further comparison the theoretical carrier concentration (N_{th}), which is calculated using the lattice parameters (table 1) with the assumption of charge carriers only in a half-filled d band given by TaS_2 and NbS_2 (i.e. Ta and Nb in the +4 state), is listed in table 3. Comparing N_{th} with N_{exp} it can be

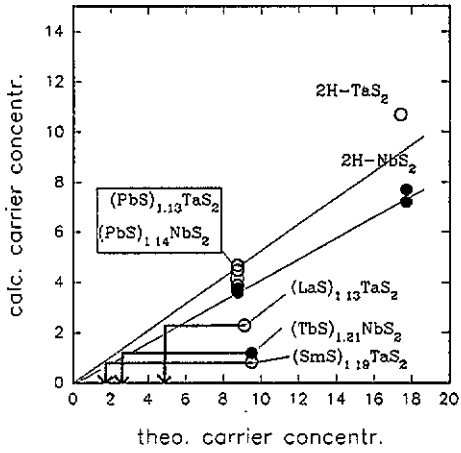

Figure 8. The experimental carrier concentration (N_{exp}, equation (4) with $m^* = 1$) as a function of the theoretically expected number of carriers (N_{th}) in units of $\times 10^{27}$ m^{-3}. For details see the text and table 3. For 2H-NbS_2 and 2H-TaS_2 the data for N_{est} as given in table 3 are used. The lines are a guide for the eye and indicate the possible values, assuming effective masses of $m^* \simeq 2$–2.3 (and $\epsilon_\infty \simeq 9$–11). Accordingly, the arrows mark the effective (Drude) charge carrier concentration for the La, Tb and Sm compounds, assuming the same relevant band structure as given for PbS misfit layer compounds.

deduced that the effective mass amounts to about 2–2.5 for the PbS compounds and for 2H-NbS_2, and about 1.6 for 2H-TaS_2, i.e. $m^* = m_r$ (the ratio given in table 3). However, for compounds with La, Sm and Tb, a reduced effective carrier concentration is indicated, assuming effective masses equal to those obtained for the MLCs with M = Pb, Sn.

The results are demonstrated more clearly in figure 8. Shown are the data points for N_{exp} plotted against N_{th} from table 3. Included also are the data points for 2H-NbS_2 and 2H-TaS_2. The lines are a guide to the eye. they cut the possible field of expected carrier concentrations, assuming the same effective masses ($m^* \simeq 2$–2.3) for all the misfit layer compounds presented. The graph shows in this case an effective carrier concentration of about 5×10^{27}, 2.5×10^{27} and 2.0×10^{27} m^{-3} for $(LaS)_{1.13}TaS_2$, $(TbS)_{1.21}NbS_2$ and $(SmS)_2TaS_2$, respectively. Hall effect data for these compounds show a number of holes (at $T = 300$ K) of 1.2×10^{27} [38], 1.6×10^{27} [27] and 0.5×10^{27} [21] m^{-3}, using a single type of carrier picture. It can be suggested from the optical data that for $(PbS)_{1.13}TaS_2$ and $(PbS)_{1.14}NbS_2$ there is no electron donation in the stoichiometric and defect-free samples, although Hall effects indicate here a larger scatter of charge carrier concentration for the half-filled band situation, i.e. for $(PbS)_{1.13}TaS_2$: $n(\text{Hall}) = 6.3 \times 10^{27}$ m^{-3} [19] and for $(PbS)_{1.13}NbS_2$: $n(\text{Hall}) = 2.5 \times 10^{27}$ m^{-3} [11] (data at 300 K), which should be compared with N_{th} in table 3. This can be understood from the equal number of holes and electrons for these cases, which makes the Hall measurements more difficult to use in the simple single type of carrier picture.

There is also some indication, using the carrier concentrations obtained here, that the Ta-MLCs tend to smaller effective masses, compared with the Nb analogues. This agrees well with the lower effective mass for 2H-TaS_2 as compared with 2H-NbS_2.

Finally, it has been shown that the optical–near-infrared–reflection behaviour of the (Ta, Nb)S_2 misfit layer compounds can be described within the ordinary Drude assumption. The question arises as to how these data compare with known transport data. Within the Drude

model the DC conductivity (for $\omega = 0$) is related to the optical properties by

$$\sigma_0(\text{opt}) = \epsilon_\infty \omega_p^2 \epsilon_0 / \gamma \tag{8}$$

($\epsilon_0 = 8.85 \times 10^{-12}$ A s V^{-1} m^{-1}). For comparison, the obtained values for $1/\sigma_0$ using equation (8) are given in table 4, together with the observed DC resistivities. A very reasonable agreement between the data is given. A still better agreement cannot be expected because the two experiments weight the electron states in different ways.

Table 4. The 'Drude' resistivity parallel to the (100) plane expected using the Drude fit parameter ω_p and γ (equation (8), $1/\sigma_0$ (opt)) compared with the resistivity at $\omega = 0$ ($1/\sigma_{DC}$) measured in four-probe geometry (room temperature data from references as given (compare also the list in reference [23]), anisotropy neglected).

Composition	$1/\sigma_0$ (opt) (Ω m)	$1/\sigma_{DC}$ (Ω m)	Ref. for σ_{DC}
$(PbS)_{1.14}NbS_2$	2.5×10^{-6}	3.2×10^{-6}	[11]
$(TbS)_{1.21}NbS_2$	6.2×10^{-6}	2.5×10^{-6}	[23,27]
$(PbS)_{1.13}TaS_2$	2.7×10^{-6}	1.6×10^{-6}	[19]
$(LaS)_{1.13}TaS_2$	2.9×10^{-6}	2.7×10^{-6}	[23,38]
$(SmS)_{1.19}TaS_2$	7.9×10^{-6}	5.0×10^{-6}	[21]

4. Concluding remarks

The misfit layer compounds $(MS)_nTS_2$ are a new class of material yielding two lattices of the (MS) and TS_2 parts, which are incommensurate along the [100] direction. It is still unknown how these kinds of structure interact for chemical bonding, and there is presently no band structure calculation available.

Considering the core levels first investigated by Ohno [39] using x-ray absorption spectroscopy a higher amount of charge transfer from PbS and SnS to the NbS_2 layers for $(PbS)_{1.14}NbS_2$ and $(SnS)_{1.17}NbS_2$, respectively, is indicated, compared e.g. with $(LaS)_{1.13}NbS_2$. Ohno [39] suggests therefore a higher interlayer interaction for the former. X-ray photoemission data reported by Ettema *et al* [40–43] observe a nearly ideal superposition of the valence bands of both lattices for MLCs with SnS and PbS, suggesting no significant amount of charge transfer. Considering the low-energy (near-Fermi energy) behaviour the present study shows a strong reduction in the position of the free carrier plasma frequency for the La, Sm and Tb compounds compared with the Pb analogues (and also Sn). Therefore, we can say that for the La, Tb and Sm misfit layer compounds, there is strong charge transfer into the conduction band composed dominantly of d_z^2 orbitals of Ta and Nb. The effect observed is similar to that reported by Parkin and Beal [24] for the d-metal intercalates of Nb- and Ta-dichalcogenides. By doping, the number of holes in this band is reduced to $h = 1 - x \times e$, with x being the number of electrons effectively transferred. The data presented (table 3 and figure 8) indicate for La, Sm and Tb compounds (using effective masses of 2–2.3), that x is about 0.5, 0.82 and 0.76, respectively. According to x-ray absorption spectra [43] the occupation of the 4f shell of La, Sm or Ce in the misfit layer compounds corresponds to La^{3+} ($4f^0$), Sm^{3+} ($4f^5$) and Ce^{3+} ($4f^1$) species. Therefore the

presented data indicate a remaining amount of electrons, which could occupy 5d states in the La, Sm and Tb MLCs. For MLCs with M = Pb, Sn the presented data imply no charge transfer into the conduction band of the TS_2 part. From this point of view this could indicate that the Pb and Sn MLCs are somewhat less stable compared with their La, Tb and Sm analogues.

Another question concerns the possible anisotropy in the physical properties (such as conductivity) of the (incommensurable) [100] lattice direction with respect to the [010] one. The results presented indicate an anisotropy in the effective masses, which can be explained by the slight orthorhombicity of the TS_2 sublattice alone.

In conclusion this study has shown for the first time a (small) anisotropy in the dynamic conductivity of misfit layer compounds (here with M = Pb, Sn and T = Nb, Ta) in the highly conducting (001) lattice plane. Using a single type of carrier picture (holes) confirms the charge transfer effect of La, Sm and Tb and shows optical effective masses of about 2–2.3 for the various MLCs, including 2H-NbS_2.

Acknowledgments

We would like to thank the EC for the financial support for this project (EC contract SCI*0496-C). The reflection measurements were carried out at the Department of Mineralogy at the University of Hannover, Germany. The FTIR apparatus used has been supported in a BMFT Project (F+E 13N5738), which we gratefully acknowledge.

References

[1] Sterzel W and Horn J 1970 *Z. Anorg. Allg. Chem.* **376** 254
[2] Schmidt L 1970 *Phys. Lett.* **31A** 551
[3] Schmidt L, McCarthy S L and Maita J P 1970 *Solid State Commun.* **8** 254
[4] Takahashi T, Oka T, Yamada O and Ametani K 1971 *Mater. Res. Bull.* **6** 173
[5] van Maaren M H 1972 *Phys. Lett.* **40A** 353
[6] Takahashi T, Osaka S and Yamada O 1973 *J. Phys. Chem. Solids* **43** 1131
[7] Donohue P C 1975 *J. Solid State Chem.* **12** 80
[8] Kato K, Kawada I and Takahashi T 1977 *Acta Crystallogr.* B **33** 3437
[9] Wiegers G A *et al* 1989 *Solid State Commun.* **70** 409
[10] Meetsma A, Wiegers G A, Haange R J and de Boer J L 1989 *Acta Crystallogr.* A **45** 285
[11] Wiegers G A, Meetsma A, Haange R J and de Boer J L 1989 *Solid State Ion.* **32/33** 183
[12] van Smaalen S 1989 *J. Phys.: Condens. Matter* **1** 2791
[13] Wiegers G A, Meetsma A, Haange R J, van Smaalen S, de Boer J L, Meerschaut A, Rabu P and Rouxel J 1990 *Acta Crystallogr.* B **46** 324
[14] Wiegers G A, Meetsma A, van Smaalen S, Haange R J and de Boer J L 1990 *Solid State Commun.* **75** 689
[15] van Smaalen S 1991 *J. Phys.: Condens. Matter* **3** 1247
[16] van Smaalen S 1992 *Mater. Sci. Forum* **100/101** 173
[17] van Smaalen S and de Boer J L 1992 I *Phys. Rev.* B **46** 2750
[18] Wiegers G A, Meetsma A, Haange R J and de Boer J L 1988 *Mater. Res. Bull.* **23** 1551
[19] Wulff J, Meetsma A, van Smaalen S, Haange R J, de Boer J L and Wiegers G A 1990 *J. Solid State Chem.* **84** 118
[20] Wiegers G A and Haange R J 1990 *J. Phys.: Condens. Matter* **2** 455
[21] Wiegers G A, Meetsma A, Haange R J and de Boer J L 1991 *J. Less-Common Met.* **168** 347
[22] Wiegers G A and Haange R J 1991 *Eur. J. Solid State Inorg. Chem.* **28** 1071
[23] Wiegers G A and Meerschaut A 1992 *Mater. Sci. Forum.* **100/101** 101
[24] Parkin S S P and Beal A R 1980 *Phil. Mag.* B **42** 627
[25] Sudharsanan R, Bardhan K K, Clayman B P and Irwin J C 1987 *Solid State Commun.* **62** 563
[26] Rüscher C H 1993 unpublished

[27] Zhou W Y and Wiegers G A 1993 unpublished
[28] Wulff J and Wiegers G A 1993 unpublished
[29] Jelliniek F, Bauer G and Muller H 1960 *Nature* **376** 4710
[30] Dunn J and Glaunsinger W 1988 *Solid State Ion.* **27** 285
[31] Meetsma A, Wiegers G A, Haange R J and de Boer J L 1990 *Acta Crystallogr.* C **46** 1598
[32] Beal A R, Hughes H P and Liang W Y 1975 *J. Phys. C: Solid State Phys.* **8** 4236
[33] Liang W Y 1973 *J. Phys. C: Solid State Phys.* **6** 551
[34] Beal A R 1978 *J. Phys. C: Solid State Phys.* **11** 4583
[35] Ghorayeb A M, Liang W Y and Yoffe A D 1986 *J. Phys. C: Solid State Phys.* **19** 7323
[36] Rüscher C H 1993 unpublished
[37] Stern F 1963 *Solid State Phys.* **15** 350
[38] Zeinstra J T and Wiegers G A 1993 unpublished
[39] Ohno Y 1991 *Solid State Commun.* **79** 1081
[40] Ettema A R H F, Wiegers G A, Haas C and Turner T S 1992 *Surf. Sci.* **269/70** 1161
[41] Ettema A R H F and Haas C 1993 *J. Phys.: Condens. Matter* **5** 3817
[42] Ettema A R H F, Haas C and Turner T S 1993 *Phys. Rev.* B **47** 12 794
[43] Ettema A R H F 1993 *Thesis* University of Groningen